Single-tube on beam quartz-enhanced photoacoustic spectrophones exploiting a custom quartz tuning fork operating in the overtone mode

Marilena Giglio[a,b], Angelo Sampaolo[a,b], Pietro Patimisco[a,b], Huadan Zheng[b,c], Hongpeng Wu[b,c], Lei Dong[c], Frank K. Tittel[b], and Vincenzo Spagnolo[a]

[a]Dipartimento Interateneo di Fisica, University and Politecnico of Bari, CNR-IFN UOS BARI, Via Amendola 173, Bari, Italy;
[b]Department of Electrical and Computer Engineering, Rice University, 6100 Main Street, Houston, TX 77005, USA;
[c]State Key Laboratory of Quantum Optics and Quantum Optics Devices, Institute of Laser Spectroscopy, Shanxi University, Taiyuan 030006, China

ABSTRACT

We report here on the realization of a single-tube on-beam quartz-enhanced photoacoustic (QEPAS) spectroscopy sensor employing a custom-made quartz tuning fork (QTF) with a large prong spacing. The prongs of the QTF have been designed in order to provide a quality factor twice higher when the QTF operates in the first overtone flexural mode than in the fundamental mode. The influence of the microresonator tube on the main parameters characterizing the sensing performance of the QEPAS spectrophone, including the quality factor, the magnitude of the QEPAS signal and the associated background noise was investigated in detail.

Keywords: quartz tuning fork, photoacoustic spectroscopy, quantum cascade laser, gas sensing

1. INTRODUCTION

Quartz-enhanced photoacoustic spectroscopy (QEPAS) is a well-established laser-based technique for gas sensing. QEPAS offers compactness, high detection sensitivity and selectivity, utilizing a quartz-tuning fork (QTF) to transduce the sound wave produced by an absorbing gas into an electrical signal [1-5]. The QEPAS sensitivity can be further enhanced by means of acoustic amplification provided by two micro-resonator tubes and the QTF positioned between them. Until 2013, all QEPAS sensors reported in the literature made use of commercial QTFs designed for timing application to vibrate at a resonance frequency of 32,768 Hz. These QTFs have prongs 3 mm long, 0.35 mm wide and 0.34 mm thick with a prong spacing of ~0.3 mm. The QTFs have a quality factor as high as 10,000 in air, increasing up to 100,000 in vacuum. The design parameters of the two tubes, namely the inner diameter (ID), the outer diameter (OD) and the length that maximize the QEPAS response have been experimentally determined and fall in the range 0.5 mm-0.84 mm for the ID, 0.8mm-1.2mm for OD, while the length of a single tube falls in the range 3.9-5.1 mm. the QEPAS signal-to-noise ratio (SNR) was amplified up to 30 times with respect to that measured for the bare QTF using the two micro-resonator tubes [6].

Recently, custom-made QTFs with prong spacing >700 μm were implemented in QEPAS sensors. In particular, the use of custom QTFs is mandatory to extend QEPAS operation to the THz spectral range. The requirement of such custom QTFs was the necessity to have larger prong spacing. THz sources are typically characterized by long wavelengths (60-300 μm), low beam spatial qualities and high divergence angles, thus making it impossible for the laser beam to pass between the two prongs of a standard QTF, spaced by only 300 μm [7-10].

The first implementation of micro-resonator tubes with a custom-made QTF was reported in Ref. [11]. The employed tuning fork had a prong spacing of 0.8 mm and was characterized by a fundamental resonance frequency of 7205 Hz and a quality factor of 8536 at atmospheric pressure. A pair of 23 mm long tubes, whose inner diameter was 1.3 mm was employed. The gaps between the QTF and the tubes were fixed to 30 μm. The use of such micro-resonator tubes allowed a 40 times amplification of the QEPAS SNR.

Custom tuning forks also opened the way to two novel approaches to increase the sensing performance of a QEPAS spectrophone. First, QTFs with larger prongs made it possible to accommodate between them a single-tube resonator

Quantum Sensing and Nano Electronics and Photonics XIV, edited by Manijeh Razeghi,
Proc. of SPIE Vol. 10111, 1011107 · © 2017 SPIE · CCC code: 0277-786X/17/$18
doi: 10.1117/12.2252368

(SO-QEPAS), with a pair of slits realized where the acoustic pressure antinode is located. With this approach, the size of the QEPAS spectrophone was reduced with respect to a dual-tube configuration [12, 13]. Secondly, QTFs can be specifically designed to enhance the first overtone mode providing a higher quality factor with respect to the fundamental mode [14, 15].
In this work, we combined these two approaches and investigated the sensing performance of a single-tube on-beam QEPAS spectrophone exploiting a custom QTF operating in the overtone mode. We analyzed in detail how the geometry of the resonator tube influences the sensing performance of the QEPAS spectrophone.

2. CHARACTERIZATION OF THE BARE QUARTZ TUNING FORK

The geometry of the QTF prong can be designed in order to enhance the quality factor of the overtone mode with respect to the fundamental mode. The quality factor of a prong resonating in air is determined by two classes of loss mechanisms: extrinsic losses, mainly due to the damping by air and intrinsic losses mainly due to interactions with its support structure (i.e. support losses) [16, 17]. Hence, for a given resonance frequency, the quality factor of a QTF includes both loss mechanisms. For the fundamental mode, the support losses can be neglected and the quality factor can be related to the prong width w, prong length L and crystal thickness T by [15, 16]:

$$Q \sim \frac{wT}{L} \tag{1}$$

The quality factor of an overtone mode is mainly dominated by the support losses, which can be expressed for a cantilever beam by [14]:

$$Q_{supp} \sim \frac{1}{n^2}\left(\frac{L}{w}\right)^3 \tag{2}$$

Even if the support losses increase with the mode number n (n = 1.194 for the fundamental mode and 2.988 for the first overtone mode), it is possible to obtain a larger Q for the first overtone mode with respect to the fundamental one by an appropriate selection of the parameter L/w. However, when w is reduced, the extrinsic losses could start to dominate also for the overtone mode. For this reason, the best way to obtain a higher quality factor for the overtone mode is to increase the prong length, while keeping w not below 1 mm. According to these considerations, the sizes of the selected QTF are listed in Table 1.

Table 1. Dimensions of the custom tuning fork.

Prong Length L (mm)	19
Prong width w (mm)	1.4
Quartz Crystal Thickness T (mm)	0.8
Prong spacing (mm)	1

The custom-made QTF was realized starting from a z-cut quartz wafer. Standard photo-lithographic techniques were used to etch the QTFs by using a mask and chemical etching in a hydrogen fluoride solution. Cr and Au patterns were photo-lithographically defined on both sides of the wafer and applied by means of shadow masks. For the electrical characterization of the QTF, we employed the excitation and detection scheme reported in detail in [16]. A function generator was used to provide a sinusoidal voltage to the QTF. The piezoelectric current passes through a current-to-voltage converter using an operational amplifier. The output voltage is measured by a lock-in amplifier. In order to determine the QTF resonance properties and the quality factor, the frequency of the function generator was varied and processed by the lock-in output via a data acquisition card and computer. The QTF resonance curves for the fundamental and the overtone mode are shown in Fig. 1.

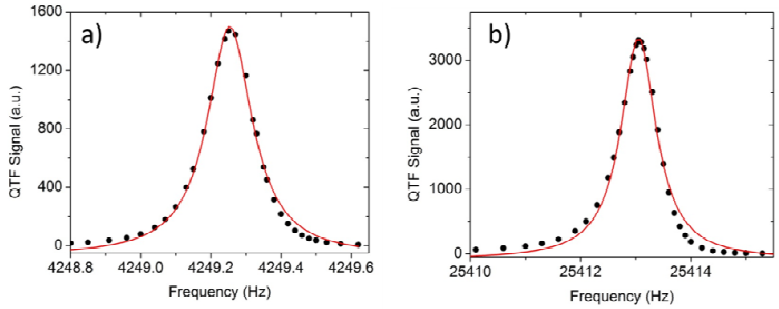

Figure 1. The QTF resonance curve (dots) of the fundamental (a) and the overtone (b) mode in air at atmospheric pressure. Solid curves are Lorentzian fits.

The QTF resonance curves were fitted using a Lorentzian function in order to extract the resonance frequency and the quality factor. The obtained values are reported in Table 2.

Table 2. Resonance frequency and quality factor for the fundamental and the overtone modes.

	Fundamental mode	***Overtone mode***
Resonance frequency (Hz)	4249.25	25413.05
Quality factor	10738	28942

The overtone mode shows a quality factor that is 2.7 times higher than that of the fundamental mode.

The architecture of the QEPAS sensor used to study the photoacoustic performances of both resonance modes is similar to that reported in [15]. We employed a single-mode quantum cascade laser (QCL) emitting at 7.7 μm as the excitation source for the QEPAS sensor. The collimated beam exiting from the laser was focused between the prongs of the QTF by using a lens with a focal length of 50 mm. The QTF is placed in a housing filled with air samples containing a fixed concentration of 1.7% of water vapor at atmospheric pressure. At a QCL current of 263 mA and a temperature of 20 °C, the laser emission wavenumber falls at 1296.49 cm^{-1}, resonant with a water line absorption having a line strength of 1.70×10^{-22} cm/mol as reported in the HITRAN database [18]. The optical power focused between the two prongs was 108 mW. All QEPAS measurements were performed by using wavelength modulation technique with *2f*-detection: a sinusoidal dither at an half of the selected QTF resonance frequency was applied to the QCL current driver, while the QTF signal was demodulated at the QTF resonance frequency by means of a lock-in amplifier [19-21]. A voltage ramp at 10 mHz was simultaneously applied to the QCL current to scan the laser optical frequency at the water absorption peak. The fundamental mode the QEPAS signal is maximized when the beam is focused between the prongs and at 1.3 mm from the top of the QTF. For the overtone mode, the largest QEPAS signal was obtained when the laser beam was positioned at 12 mm from the top. The related QEPAS scans are shown in Fig. 2.

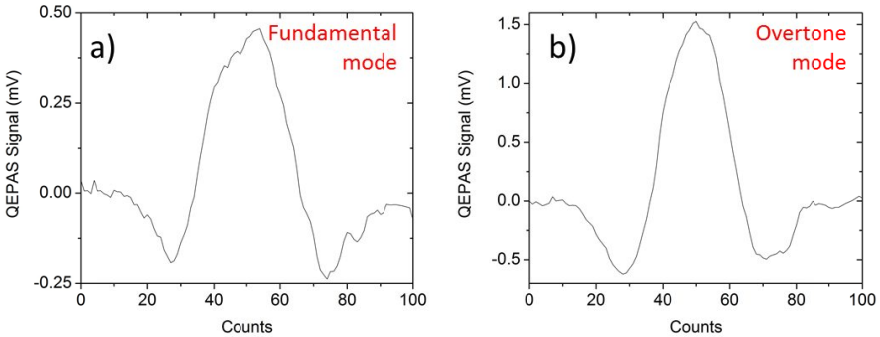

Figure 2. QEPAS spectral scans of the selected water line with the QEPAS sensor operating with both wavelength modulation and *2f*-detection with a QTF operating with the fundamental (a) and the overtone (b) mode. A slow ramp at a frequency of 10 mHz and a sine frequency of 2124.62 Hz (12706.52 Hz) were applied when the QTF fundamental (overtone) mode was selected. The integration time of the lock-in amplifier was set to 100 ms in both cases.

The peak value measured for the first overtone mode (1.53 mV) is ~ 3.3 times higher than that obtained using the fundamental mode (0.46 mV) with the same 1σ noise level of 13μV.

3. SINGLE-TUBE QEPAS

A single-tube acting as one-dimensional acoustic resonator was located between the prongs of the QTF. For tubes having an outer diameter (OD) larger than the prong spacing, the OD was reduced by polishing the waist of the tube thickness. A pair of slits was opened on each side of the tube waist, symmetrically in the middle of the tube as shown in Fig. 3.

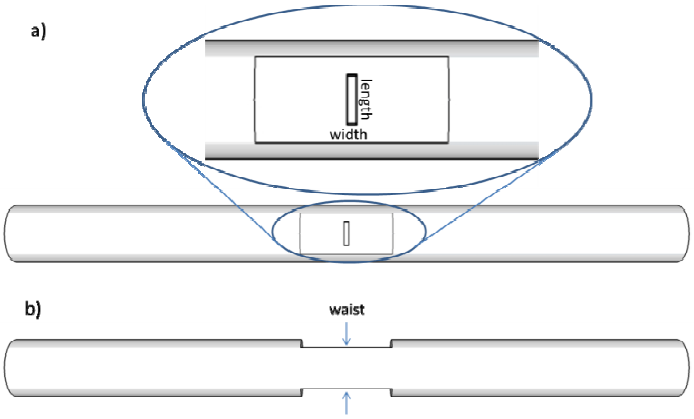

Figure 3. Front (a) and top (b) view of the single microresonator tube.

The microresonator tube was positioned between the prongs of the QTF at 12 mm from the top of the QTF in order to allow the sound wave exiting from the two slits to impact on the internal surface of the two prongs. A complete investigation of the impact of the tubes geometry, namely the internal diameter (ID), the length and the size of the slit, on the SO-QEPAS sensor performance was carried out for the QTF overtone mode.
In order to determine the optimum internal diameter maximizing the SO-QEPAS signal a set of 4 tubes having different internal diameters (0.67 mm, 0.80 mm, 0.88 mm and 0.96 mm) with the same length l = 10.8 mm was prepared. The slit length was 0.5 mm for ID = 0.67 mm and 0.80 mm, and 0.9 mm for ID = 0.88 mm and 0.96 mm. The slit width was 0.1 mm for all microresonator tubes. The QEPAS peak signal as a function of the tube ID is shown in Fig. 4.

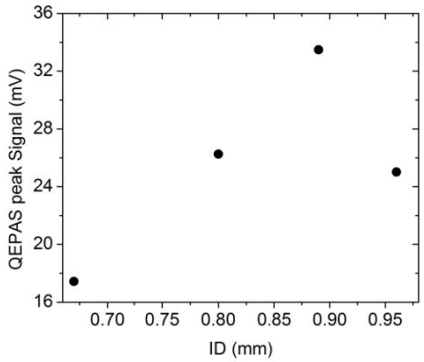

Figure 4. QEPAS peak signals plotted as a function of the internal diameter of the microresonator tube. The length of the tube was fixed to 10.8 mm.

The highest QEPAS signal (33.5 mV) was obtained with tube having ID = 0.88 mm. The QEPAS noise level is influenced by the size of the internal diameter as the radiation touching the internal surface of resonator tubes can drastically increase the QEPAS background noise level [22-24]. In Fig. 5a the 1σ noise values recorded at different IDs

was plotted and in Fig. 5b the related optical coupling efficiencies, defined as the percentage of the laser power coupled with the SO-QEPAS spectrophone is depicted.

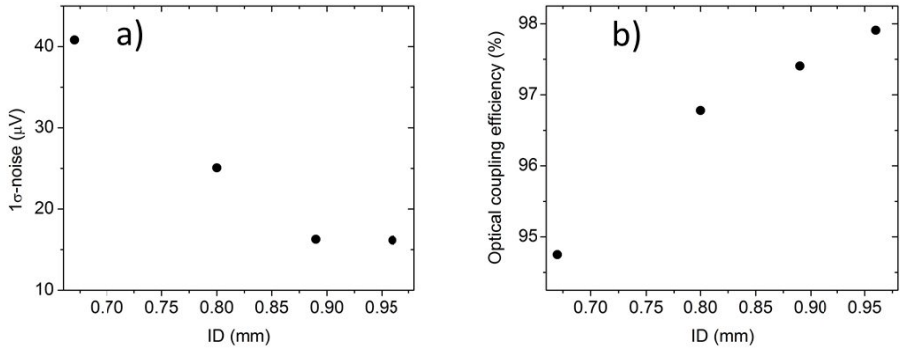

Figure 5. 1σ background noise values (a) of the QEPAS signal and the optical coupling efficiency (b) plotted as a function of the internal diameter of the microresonator tube. The length of the tube was fixed to 10.8 mm in all cases.

We observed that for an ID = 0.88 mm and l = 10.8mm the background noise level is 16.3μV, 20% higher than that measured for the bare QTF (13.0 μV). This was due to a small amount of laser power touching the tube. This was also confirmed by a reduction of the laser power coupling efficiency to 97.4 % (99.5% for the bare QTF). For the smallest ID, the noise level increases up to 40.8μV and the coupling efficiency decreases to 94.8%.
For an ID = 0.88 mm, the QEPAS performance at different tube lengths (slit sizes were not changed), ranging from 13.3 mm (~λ) to 7 mm (~λ/2) was investigated. The results are shown in Fig. 6.

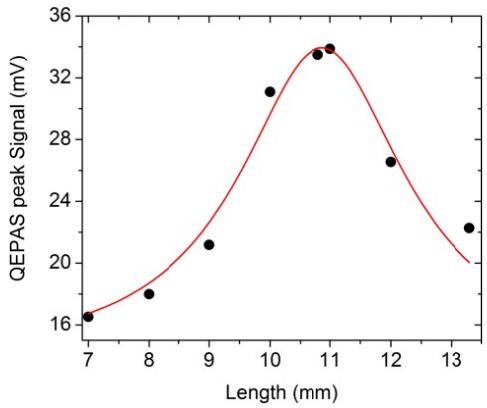

Figure 6. QEPAS peak signals (dots) plotted as a function of the microresonator tube length. The tube internal diameter was 0.88 mm in all cases. The solid line is the Lorentzian fit of the experimental data.

The maximum QEPAS signal of 33.9 mV was obtained for an optimal tube length of 11.0 mm. The observation of an optimal tube length > λ/2 is a clear evidence that the 1st harmonic acoustic standing waves in the tube were partially distorted by the two slits present in the acoustic resonator, as observed in previous SO-QEPAS experiments [12, 13]. In Fig. 7 we depict the 1σ background noise values and the related coupling efficiency as a function of the microresonator tube length.

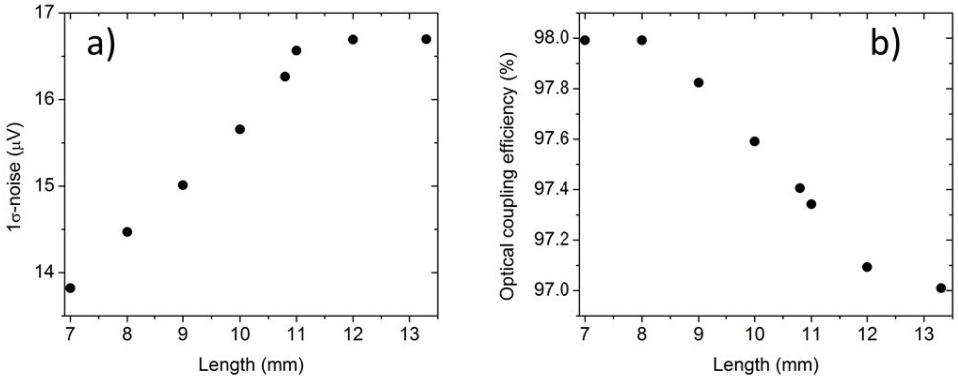

Figure 7. 1σ background noise values (a) of the QEPAS signal and optical coupling efficiency (b) plotted as a function of the microresonator tube length. The tube internal diameter was 0.88 mm in all cases.

The optical coupling reaches 98% and the noise level is 13.8 μV, which is almost identical to that measured with the bare QTF when the length of the microresonator tube is reduced to 7mm. For a tube length l = 11 mm, the noise level is 16.6 μV.

The last geometrical parameter to be investigated was the slit size. For the ID = 0.88 mm and an l = 10.8 mm we enlarged the slit width without changing its length. The results are shown in Fig. 8.

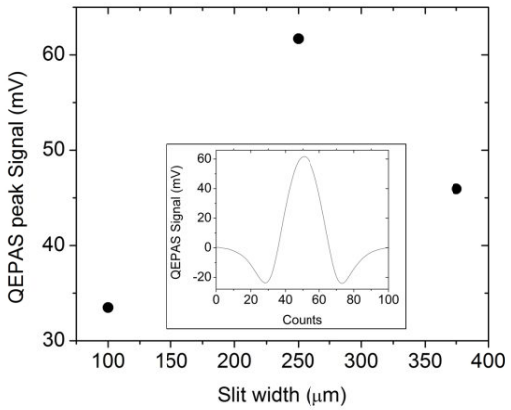

Figure 8. QEPAS peak signal recorded for three different slit widths. In all three cases, the tubes were 10.8 mm long, with the ID of 0.88 mm and the slit length of 0.9 mm. Inset: SO-QEPAS spectral scan of the selected water line with the QTF operating with the overtone mode with the tube ID of 0.88 mm, length of 11.0 mm and a slit width of 250μm. The integration time of the lock-in amplifier was set to 100 ms.

The QEPAS signal increases up to 61.7 mV when the slit width is 250 μm, almost twice with respect to a slit width of 100 μm. The quality factor was ~26,000, ~10% lower than that of the bare QTF. The QEPAS signal decreases to 45.9 mV when the slit width is enlarged to 370 μm.

4. CONCLUSIONS

In this work, we demonstrated a SO-QEPAS spectrophone configuration using a single stainless tube and a custom tuning fork, in which a single tube microresonator was inserted between the prongs of the QTF. We investigated the influence of the geometry of the microresonator tube, including the internal diameter, the length and the slit width on the QEPAS sensor performance when the QTF operates in the first overtone mode. The QEPAS sensor system operated in the mid-infrared spectral range by using a quantum cascade laser emitting at 7.7 μm to target the water absorption. The optimum geometrical parameters of the tube maximizing the QEPAS signal were internal diameter of 0.88 mm, length of

11.0 mm and a slit width of 250μm. With these conditions, we measured a SO-QEPAS signal 40 times higher with respect to a bare QTF. An additional improvement in QEPAS sensitivity can be obtained by using a novel QEPAS spectrophone composed of two acoustic resonators operating at the two antinodes of the overtone mode and employing a double-pass beam configuration. Furthermore, since the optimal gold contact configuration for the 1st overtone flexural mode polarity requires changes of the electrodes along the prongs, obtainable by an octupole gold pattern configuration, additional enhancement of the QEPAS SNR can be expected by employing this type of QTF electrode design.

ACKNOWLEDGEMENTS

Frank Tittel acknowledges support by the Welch Foundation (Grant R4925S). The authors from Dipartimento Interateneo di Fisica di Bari acknowledge financial support from two Italian research projects: PON02 00675 and PON02 00576. The authors from Shanxi University acknowledges the support by National Natural Science Foundation of China 61622503, the Education Innovation Project of Shanxi Province (2016BY028).

REFERENCES

[1] Patimisco, P., Scamarcio, G., Tittel, F.K., Spagnolo, V., "Quartz-Enhanced Photoacoustic Spectroscopy: A Review," Sensors 14, 6165-6206 (2014).
[2] Kosterev, A.A., Tittel, F.K., Serebryakov, D., Malinovsky, A., and Morozov, A., "Applications of quartz tuning fork in spectroscopic gas sensing," Rev. Sci. Instrum. 76, 043105:1–043105:9 (2005).
[3] De Cumis, M. S., Viciani, S., Borri, S., Patimisco, P., Sampaolo, A., Scamarcio, G., De Natale, P., D'Amato, F., and Spagnolo, V., "Widely-tunable, mid-infrared fiber-coupled quartz-enhanced photoacoustic sensor for environmental monitoring," Opt. Express 22, 28222-28231 (2014).
[4] Ren, W., Jiang, W., Sanchez, N. P., Patimisco, P., Spagnolo, V., Zah, C.-E., Xie, F., Hughes, L. C., Griffin, R. J., and Tittel, F. K., "Hydrogen peroxide detection with quartz-enhanced photoacoustic spectroscopy using a distributed-feedback quantum cascade laser," Appl. Phys. Lett. 104, 041117 (2014).
[5] Jahjah, M., Jiang, W., Sanchez, N. P., Ren, W., Patimisco, P., Spagnolo, V., Herndon, S.C., Griffin, R. J., and Tittel, F. K., "Atmospheric CH_4 and N_2O measurements near Greater Houston area landfills using a QCL-based QEPAS sensor system during DISCOVER-AQ 2013," Opt. Letters 39, 957-960 (2014).
[6] Dong, L., Kosterev, A. A., Thomazy, D., and Tittel, F. K., "QEPAS spectrophones: design, optimization, and performance," Appl. Phys. B 100, 627-635 (2010).
[7] Borri, S., Patimisco, P., Sampaolo, A., Beere, H.E., Ritchie, D.A., Vitiello, M.S., Scamarcio, G., and Spagnolo, V., "Terahertz quartz enhanced photo-acoustic sensor," Appl. Phys. Lett.103, 021105 (2013).
[8] Patimisco, P., Borri, S., Sampaolo, A., Beere, H.E., Ritchie, D.A., Vitiello, M.S., Scamarcio, G., and Spagnolo, V., "A quartz enhanced photo-acoustic gas sensor based on a custom tuning fork and a terahertz quantum cascade laser," Analyst 1339, 2079-2087 (2014).
[9] Spagnolo, V., Patimisco, P., Pennetta, R., Sampaolo, A., Scamarcio, G., Vitiello, M.S., and Tittel, F.K., "THz Quartz-enhanced photoacoustic sensor for H_2S trace gas detection," Opt. Express 23, 7574-7582 (2015).
[10] Sampaolo, A., Patimisco, P., Giglio, M., Vitiello, M.S., Beere, H.E., Ritchie. D.A., Scamarcio, G., Tittel, F. K., and Spagnolo, V., "Improved Tuning Fork for Terahertz Quartz-Enhanced Photoacoustic Spectroscopy," Sensors, 16, 439 (2016).
[11] Wu, H., Sampaolo, A., Dong, L., Patimisco, P., Liu, X., Zheng, H., Yin, X., Ma, W., Zhang, L., Yin, W., Spagnolo, V., Jia, S., and Tittel, F. K., "Quartz enhanced photoacoustic H_2S gas sensor based on a fiber-amplifier source and a custom tuning fork with large prong spacing," Appl. Phys. Lett. 107, 111104 (2015).
[12] Zheng, H., Dong, L., Sampaolo, A., Wu, H., Patimisco, P., Yin, X., Ma, W., Zhang, L., Yin, W., Spagnolo, V., Jia, S., and Tittel, F. K., "Single-tube on-beam quartz-enhanced photoacoustic spectroscopy," Opt. Lett. 41, 978-981 (2016).
[13] Zheng, H., Dong, L., Sampaolo, A., Wu, H., Patimisco, P., Ma, W., Zhang, L., Yin, W., Xiao, L., Spagnolo, V., Jia, S., and Tittel, F. K., "Overtone resonance enhanced single-tube on-beam quartz enhanced photoacoustic spectrophone, " Appl. Phys. Lett. 109, 111103 (2016).

[14] Sampaolo, A., Patimisco, P., Dong, L., Geras, A., Scamarcio, G., Starecki, T., Tittel, F. K., and Spagnolo, V., "Quartz-enhanced photoacoustic spectroscopy exploiting tuning fork overtone modes," Appl. Phys. Lett. 107, 231102 (2015).
[15] Tittel, F.K., Sampaolo, A., Patimisco, P., Dong, L., Geras, A., Starecki, T., and Spagnolo, V., "Analysis of overtone flexural modes operation in quartz-enhanced photoacoustic spectroscopy," Opt. Express 24, A682-A692 (2016).
[16] Patimisco, P., Sampaolo, A., Dong, L., Giglio, M., Scamarcio, G., Tittel, F.K., and Spagnolo, V., "Analysis of the electro-elastic properties of custom quartz tuning forks for optoacoustic gas sensing," Sensor Actuat. B-Chem. 227, 539-546 (2016).
[17] Hao, Z., Erbil, A., and Ayazi, F., "An analytical model for support loss in micromachined beam resonators with in-plane flexural vibrations," Sensors Actuat. A-Phys. 109, 156-164 (2003).
[18] http://www.hitran.org/
[19] Schilt, S., Thévenaz, L., and Robert, P., "Wavelength modulation spectroscopy: combined frequency and intensity laser modulation," Appl. Opt. 42, 6728–6738 (2003).
[20] Bidaux, Y., Bismuto, A., Patimisco, P., Sampaolo, A., Gresch, T., Strubi, G., Blaser, S., Tittel, F. K., Spagnolo, V., Muller A., and Faist, J., "Mid infrared quantum cascade laser operating in pure amplitude modulation for background-free trace gas spectroscopy," Opt. Express 24, 26464-26471 (2016).
[21] Patimisco, P., Sampaolo, A., Bidaux, Y., Bismuto, A., Scott, M., Jiang, J., Muller A., Faist, J., Tittel, F. K., and Spagnolo, V., "Purely wavelength- and amplitude-modulated quartz-enhanced photoacoustic spectroscopy," Opt. Express 24, 25943-25954 (2016).
[22] Giglio, M., Patimisco, P., Sampaolo, A., Scamarcio, G., Tittel, F. K., and Spagnolo, V., "Allan Deviation Plot as a Tool for Quartz-Enhanced Photoacoustic Sensors Noise Analysis," IEEE Trans. Ultrason. Ferroelect. Freq. Control, 63, 555-560 (2016).
[23] Dong, L., Spagnolo, V., Lewicki, R., and Tittel, F. K., "Ppb-level detection of nitric oxide using an external cavity quantum cascade laser based QEPAS sensor," Opt. Express 19, 24037-24045 (2011).
[24] Spagnolo, V., Patimisco, P., Borri, S., Scamarcio, G., Bernacki, B.E., and Kriesel, J., "Mid-infrared fiber-coupled QCL-QEPAS sensor," Appl. Phys. B 112, 25-33 (2013).